Dynamic hydrological niche segregation: how plants compete for water in a semiarid ecosystem

Ying Zhao[1,2,5], Li Wang[1,2*], Kwok P. Chun[3], Alan D. Ziegler[4], Jaivime Evaristo[5*]

[1]College of Natural Resources and Environment, Northwest A&F University, Yangling, Shaanxi, China

[2]Institute of Soil and Water Conservation, Chinese Academy of Sciences and the Ministry of Water Resources, Yangling, Shaanxi, China

[3]Department of Geography and Environmental Management, University of the West of England, Bristol, UK

[4]Faculty of Fishery Technology and Aquatic Resources, Mae Jo University, Chiang Mai, Thailand

[5]Copernicus Institute of Sustainable Development, Utrecht University, Utrecht, the Netherlands

Corresponding authors:

Li Wang, Institute of Soil and Water Conservation, Northwest A&F University

E-mail: wangli5208@nwsuaf.edu.cn

Jaivime Evaristo, Copernicus Institute of Sustainable Development, Utrecht University

E-mail: j.evaristo@uu.nl

Abstract

Hydrological niche segregation (HNS), which refers to differences in root water uptake depth and physiological traits among coexisting species, remains poorly understood especially with respect to moisture changes and diverse water use strategies. This is particularly the case in regions with a seasonally dry climate where plants must constantly adapt to water stress. Over a 2-year period, we analyzed the isotopic compositions of xylem and soil water (δ^2H, $\delta^{18}O$) and foliar $\delta^{13}C$ to identify the water sources and intrinsic water use efficiency (WUEi), respectively, of four coexisting plant species. These species include *Populus simonii* (a type of tree), *Caragana korshinskii* and *Salix psammophila* (both types of shrub), and *Artemisia ordosica* (a semi-shrub). This study was conducted in a semi-arid ecosystem in China's Loess Plateau (CLP). To quantify HNS defined by δ^2H, $\delta^{18}O$ and $\delta^{13}C$, we used a model called nicheROVER. Our results show that these four co-existing species had distinct position on a hydrological niche axis defined by their water sources and WUEi. *P. simonii* depended on deep soil water and demonstrated a high WUEi. Both shrubs, *C. korshinskii* and *S. psammophila*, utilized deep and intermediate soil water, respectively, and had comparable WUEi. The semi-shrub *A. ordosica* relied on shallow soil water and showed a low WUEi. These differences in water sources and WUEi led to HNS between *A. ordosica* and the other three species during the wet year. However, in a dry year, HNS reduced as the shrubs and semi-shrub increased their use of deep soil water and

improved WUEi. Overall, these results demonstrate that HNS is a dynamic process that varies on at least an annual basis. It expands and contracts as plants regulate their water uptake and loss in response to changing soil moisture conditions.

Keywords: hydrological niche segregation; plant water uptake; water stress management; Loess Plateau; stable isotopes; nicheROVER

1. Introduction

Water is the most limiting resource for plant survival and growth in arid and semi-arid ecosystems. Coexisting plant species usually adopt diverse water use strategies (e.g., root biomass adjustment, shift in root water uptake depth, stomatal regulation) to compete for or apportion this limited resource (Granda et al., 2022; Kulmatiski et al., 2020b; Rodríguez-Robles et al., 2020). Silvertown et al. (2015) introduced the concept of hydrological niche segregation (HNS) concerning the apportionment of soil water resources in a plant community. HNS comprises three aspects: (a) partitioning of space along fine-scale moisture gradients; (b) partitioning of water as a resource; and/or (c) partitioning of recruitment opportunities due to species specializing in certain patterns of temporal water supply or storage variance.

HNS theory has found applications in a plethora of environments such as wet meadows, coastal dune slacks, tropical rainforests, savannas, and Mediterranean climates (Araya et al., 2011; Bartelheimer et al., 2010; Camarero et al., 2018; Case et al., 2020; Dwyer et al., 2021; Holdo & Nippert, 2022; Kulmatiski et al., 2020a; Matos

et al., 2022; Wu et al., 2022). A common thread in these studies is that root distributions in the soil can cause variability in soil water resources available to different plants. Walter's two-layer hypothesis (1939) posits that trees and grasses coexist by exploiting different soil water depths: trees access deep soil water with their deep roots while grasses, with their shallow roots, utilize near-surface soil water (Ward et al., 2013). A recent study on a savanna ecosystem corroborates this by demonstrating how grasses' shallow roots provide rapid access to sufficient soil water, enabling constant grass cover, while trees' slightly deeper roots access more water throughout the soil profile under most conditions (Kulmatiski & Beard, 2022).

HNS among coexisting species, influenced by differences in root distribution, is evident not only in spatially segregated deep and shallow water sources but also in temporal segregation due to differences in soil water age. This is known as "root-niche separation", where deep-rooted vegetation uses water stored from wet-season precipitation during the dry season, while more shallow-rooted species directly access dry-season precipitation (Ivanov et al., 2012).

Another significant aspect of HNS is the differentiation of physiological traits related to water loss management through the stomata of coexisting species (Camarero et al., 2018; Rodríguez-Robles et al., 2020). Stomate play a critical role in managing the trade-off between water conservation and carbon assimilation (hence growth) as they close to reduce water loss during transpiration, simultaneously limiting CO_2 uptake (Seibt et al., 2008). This trade-off between carbon acquisition and water conservation along fine-scale ecophysiological gradients likely contributes to HNS among coexisting

species (Silvertown et al., 2015). For example, Moreno-Gutiérrez et al. (2012) found that 10 co-existing plant species in a Mediterranean ecosystem exhibited diverse stomatal regulation and water use strategies. Some were "opportunistic" with high stomatal conductance and low WUEi; others "conservative", having low stomatal conductance and high WUEi. The ecophysiological niche segregation was observable in foliar $\delta^{18}O$ and $\delta^{13}C$ data.

Previous studies have used root depth, access to light, tolerance of low water potential (Brum et al., 2019), or radial growth and WUEi (Camarero et al., 2018) to define hydrological niche axes of co-existing species. Overall, HNS pertains to the capacity of different species to coordinate water uptake from the soil profile and management of water loss through stomata. HNS has been widely evaluated through a wide spectrum of stomatal behaviours and contrasting water use strategies among coexisting plant species, but these studies tend to assess HNS qualitatively based on differences in root water uptake depth or physiological characteristics (Guderle et al., 2018; Rodríguez-Robles et al., 2020). To our knowledge, research to date has not generally been able to quantify the dynamics of HNS between species under the dual control of water acquisition via roots and water loss through stomata, which is the focus of our study for a semiarid ecosystem.

In this study, we aim to characterize the water use strategies and HNS of four coexisting plant species (*Populus simonii* (tree), *Caragana korshinskii* (shrub), *Salix psammophila* (shrub), and *Artemisia ordosica* (semi-shrub)) in a semiarid ecosystem in CLP. We used traditional, isotopic, and modelling approaches to identify water sources,

calculate WUEi and water stress, and confirm HNS in both wet and dry years. We formulated three hypotheses: (1) the four target plant species have distinct water uptake depths and physiological regulations; (2) there is clear HNS among the species; and (3) HNS is dynamic as plants adjust their water use based on changing soil moisture patterns annually.

2. Materials and methods

2.1. Study area

The study was conducted in the Liudaogou Catchment (38°47′-38°49′N, 110°21′-110°23′E), which is located on the southern edge of the Mu Us Sandy Land, in Shaanxi province of China (Fig. 1a). The catchment is part of the Grain for Green project, which was launched in 1999 to combat erosion on the Loess Plateau and sediment buildup in the Yellow River (Chen et al., 2015). The Liudaogou Catchment is about 6.89 km^2 and ranges in altitude from 1094 m to 1274 m. The regional climate is classified as semi-arid due to low annual rainfall and strong seasonal variations in moisture (Fu et al., 2017; Tsunekawa et al., 2014). The average annual precipitation is 464 ± 121 mm based on data from 2003 to 2019 (Zhao et al., 2022). Most of the annual precipitation, 70-80%, falls from June to August, while winter snowfall (December-February) is only about 10 mm on average based on data from 2003 to 2019.

Surficial soil in the study area has evolved from material transported by strong storms from distant northwest locations throughout the Quaternary (Fu et al., 2017; Liu, 1985). The relief of the underlying parent material is relatively flat, but details are

133 masked by the deposition of both ancient (Pleistocene) and contemporary eolian sands
134 (Zhang et al., 1993). Our experimental plot was located in flat sandy areas and the soil
135 is sand (USDA classification): the material in the 0-300 cm layer is composed of 95.7%
136 sand, 3.2% silt, and 1.1% clay (Fig. 1b). Relatively uniform particle composition
137 greatly reduces the potential impact of spatial heterogeneity of soil water on this study.

138 Native plants are scarce at the site, except for a few surviving shrub species such
139 as *Artemisia ordosica* Krasch, *Xanthoceras sorbifolium* Bunge, and *Ulmus macrocarpa*
140 Hance (Yuan et al., 2017). Vegetation coverage has increased significantly due to the
141 Three-North Shelter Forest and the Grain for Green programs (Lu et al., 2018).
142 Common species used in the reforestation include *Populus simonii* Carr., *Salix*
143 *matsudana* Koidz., *Salix psammophila*, and *Caragana korshinskii* Kom. Initial
144 afforestation activities mainly involved replanting forest species (Cao, 2008). These
145 restored forests then evolved into tree-shrub complex ecosystems (Cao et al., 2010,
146 2011).

147 Apricot plum trees (*P. simonii*, also known as Simon plum) were planted in our
148 study location about 40 years ago over an area of 40 hectares. Over time, three
149 understory species - Korshinsk pea (*C. korshinskii*), xerophytic shrub (*S.*
150 *psammophila*), and a dwarf, sand-binding semi-shrub (*A. ordosica*) - have emerged due
151 to seed dispersal by wind and birds (Fig. 1c). Vegetation characteristics for the four
152 species were determined within a one-hectare (100 m × 100 m) survey plot. The plot
153 was divided into twenty-five 20 m × 20 m square quadrats, inside which we established
154 nine 400-m^2 tree sub-plots, located at all locations of the diagonals of the one-hectare

155 plot (Kang et al., 2007). Every 400-m^2 quadrat was evenly divided into twenty-five 4
156 m × 4 m sub-quadrats. As before with the trees, we then investigated nine shrub sub-
157 squares located diagonally of the quadrats. A total of nine tree quadrats and eighty-one
158 shrub sub-quadrats were used to analyze the morphological characteristics of trees and
159 three shrubs, respectively. *A. ordosica* is the most abundant, with 3356 individuals per
160 hectare. The densities of *P. simonii*, *C. korshinskii*, and *S. psammophila* are much
161 lower, at 519, 494, and 301 individuals per hectare, respectively. *P. simonii* is the tallest
162 of these species, with a mean height of about 5.2 m, while *C. korshinskii*, *S.*
163 *psammophila*, and *A. ordosica* have mean heights of 1.36 m, 1.43 m, and 0.52 m,
164 respectively (Table 1).

165 *2.2. Meteorological Data*

166 Precipitation and air temperature (with 30-min resolution) data were obtained from
167 a weather station located about 1500 m from the sampling plot. Precipitation was
168 measured using TE525 rain gauges (Campbell Scientific Inc.), which has an accuracy
169 of ± 1 percent. The air temperature was measured using HMP45D probes, which have
170 ± 0.2 °C accuracy (Vaisala Inc.).

171 *2.3. Root excavations and measurements*

172 In September 2019, we collected samples of fine roots (≤ 2 mm diameter) from
173 four plant species (*P. simonii*, *S. psammophila*, *C. korshinskii* and *A. ordosica*) to
174 identify their root distributions. We first dug the roots of each species in the locations
175 where only single plants grow to identify their root characteristics (e.g., size, colour,
176 odour, orientation, etc) which we later used to distinguish species in mixed plots.

According to our investigation, the roots of *A. ordosica* have a pungent odour and the roots of *S. psammophila* are dark-red. The roots of *P. simonii* and *C. korshinskii* are yellow-brown, while the former is hard and has many branches, while the latter is more flexible, and has relatively a few branches.

We then selected a sampling plot where all four plants coexist. At 0.5 m from the center of the plot, we established three soil cuboids that were 200 cm long (closest to the sampling plant), 140 cm deep, and 120 cm wide. Specifically, these three soil cuboids are at an included angle of about 120° to each other, surrounding the sampled plants in the center. Each cuboid was excavated at 20-cm intervals for a depth interval of 0-140 cm. The cuboid at each interval was evenly divided into 3 rows and 5 columns, for a total of 15 sub-cuboids (length, 40 cm; width, 40 cm; height, 20 cm, Fig. 1d-e). The sub-cuboids were excavated individually and the fine roots of all four species were collected. These fine-root samples were rinsed, dried to constant weights at 60 °C for 24 h and weighted fine-root weight of each plant species in each sub-cuboid.

2.4. Collections and measurements of water and foliar isotopes

Three fixed sites within the plot were selected to collect samples of xylem and soil water once a month from May to September 2018-2019. At each site, two mature plants for each species similar to the mean height and basal diameter of the species measured in the ecological sample survey were fixedly selected to conduct xylem samples. Bark and phloem were peeled from fully suberized branches to avoid perturbance of xylem water isotopic composition by fractionation. Pieces of the de-barked and de-leaved twigs, 30 mm long, were then immediately placed in 10-mL vials.

199 The vials were then sealed with caps and wrapped in Parafilm. These samples were kept
200 in a cool box until storage in the lab at -20°C. Three soil profiles were collected
201 simultaneously with the xylem samples in a randomised direction 100 cm from the
202 center of sampled plants using a soil auger (diameter in 50 mm). Soil samples for each
203 soil profile were obtained at 20 depths (at 10-cm intervals for a depth interval of 0-100
204 cm and at 20-cm intervals for a depth interval of 100-300 cm). The samples from each
205 layer were separated into two parts: one part was used for determining gravimetric SWC
206 using the oven-drying method (105 °C for 12 h); the other part was used for isotopic
207 determination. Soil samples for isotopic determination were immediately placed in 10-
208 mL vials that were sealed in the same manner as the xylem samples. In addition, we
209 collected disturbed soil samples at 0-300 cm depths with 20-cm intervals using a soil
210 auger for determination of particle size using a MS 2000 Laser Particle Size Analyzer
211 (Malvern Instruments, Malvern, UK).

212 We collected approximately 250 g of fresh leaves from branches of four plants of
213 each species on the south-facing part of the crown monthly from May to September,
214 2018-2019. The foliar samples were rinsed, dried to a constant mass at 60 °C for 72 h,
215 and then ground to fine a powder that would pass through a 180-μm mesh sieve (#80).
216 The samples were analyzed for $\delta^{13}C$ with a stable isotope ratio mass spectrometer
217 (Isoprime 100, Isoprime Limited Inc., Cheadle, UK) that has a precision analysis of
218 0.1‰. $\delta^{13}C$ indicates the content of ^{13}C in a foliar sample relative to the Pee Dee
219 Belemnite standard using standard per mil (‰) notation.

220 The $\delta^{2}H$ and $\delta^{18}O$ isotopic compositions of soil water from various depths (N=60

for each month) and xylem water (N=6 for each species each month) were determined with a stable isotope ratio mass spectrometer (Isoprime 100, Isoprime Limited Inc., Cheadle, UK). The precision of the analyses of H and O isotopes was 0.5 and 0.1‰, respectively. All H and O isotope ratios are expressed relative to Vienna Standard Mean Ocean Water (V-SMOW) using standard per mil (‰) notation. Prior to analysis, water was extracted from the soil and xylem (twig) samples with a LI-2100 automated vacuum distillation system (LICA Inc., Beijing, China), which is similar to cryogenic vacuum distillation systems except that it uses a compressor refrigeration unit and not liquid nitrogen (Dai et al., 2020; Zhao et al., 2021). The extraction required 180 min with a maximum allowed vacuum pressure of 1500 Pa. Soil and xylem samples were weighed immediately prior to (M_{prior}) and after extraction (M_{post}). They were again weighed after oven drying at 105 °C for 12 h (M_{oven}) to calculate the water recovery efficiency of each sample ($\frac{M_{prior}-M_{oven}}{M_{prior}-M_{post}} \times 100\%$). The mean water recovery efficiency was more than 99% for all samples.

2.5. Measurements of ψ_{md}

The ψ_{md} for four plant species (N=5 for each species each month) was determined once a month for May-September, 2018-2019. Specifically, the ψ_{md} was measured at 12:30-13:30 using a Scholander-type pressure chamber (PMS 1000, PMS Instruments Inc., Corvalis, USA).

2.6. Quantification of HNS based on δ^2H, $\delta^{18}O$ and $\delta^{13}C$ values

We used δ^2H, $\delta^{18}O$ and $\delta^{13}C$ values as input to the nicheROVER package to determine HNS. nicheROVER is a probabilistic method for determining niche region

and pairwise niche overlaps (Swanson et al., 2015). The program produces a pairwise probability the niche of one species overlaps with that of another (Swanson et al., 2015). The nicheROVER calculates the extent of overlap between two species using niche regions (N_R), which are defined as specific locations where a species has a 95% probability of being found. Uncertainty in overlap estimates was calculated using a Bayesian framework (Jackson et al., 2011; Swanson et al., 2015). This overlap is bidirectional but asymmetric. The niche overlap of species A onto species B is determined as the fraction of the intersection area between niche A and niche B over the total niche area of B, and vice versa for species B. The higher the overlap, the lower the HNS. The original application presented by Swanson et al. (2015) used three-dimensional isotope data. In our application of nicheROVER we substitute species locations with locations where plants access water in three-dimensional space in the soil profile, based on isotopic signatures.

2.7. Determining the sources of plant water

We identified three distinct soil layers (0-30 cm, 30-70 cm and 70-300 cm) based on similarities in $\delta^{18}O$ values in 2018-2019 as well as consideration of inter-month variability (see discussion in Fig. S1). We then quantified the relative contributions of potential water sources for the four plant species based on $\delta^{18}O$ and $\delta^{2}H$ values using the simmr package in R (Parnell et al., 2013). The model is fitted with a Monte Carlo Markov Chain algorithm that produces plausible solutions for each source's contribution to the content of xylem water in each sample. The mean and standard deviation of each source isotopic composition ($\delta^{2}H$ and $\delta^{18}O$) and xylem water

composition were input into the model. The simmr package also incorporates uncertainty in trophic enrichment factors into the likelihoods of source contributions. As there is no isotope fractionation during root water uptake, the trophic enrichment factors were set to 0 (Evaristo et al., 2016).

2.8. Data analysis

Significant differences ($p<0.05$) in water sources at different soil layers, foliar $\delta^{13}C$ and ψ_{md} among the four coexisting plant species in both wet and dry years, as well as the yearly variations of the above indicators for each species were identified using the bootstrap package in R. The method employed herein does not require assumptions (e.g., normal distributions, equal variances), and provides robust results in many conditions that allow it to stand as a reliable alternative to standard parametric, nonparametric, and permutation tests in small sample size studies (Dwivedi et al., 2017; Hesterberg, 2011).

3. Results

3.1. Meteorological Conditions

During the two years of study precipitation was 708 mm (2018) and 424 mm (2019), representing a wet year followed by a dry year. During the experimentation periods (May-September of both years), the seasonal distribution of precipitation was uneven, mostly concentrated in July-August: 540 mm (76%) in 2018; 220 mm (52%) in 2019 (Fig. 2a). The mean temperature ranged from 16.7 °C in May to 22.3 °C in July during the two study years. In response to variable precipitation depths, the gravimetric

soil water contents (SWC) showed seasonal and yearly variation (Fig. 2b1, c1, d1). The mean SWC values of shallow, intermediate, and deep layers in 2018 (3.1%, 3.6% and 3.7%, respectively) were higher than in 2019 (2.1%, 2.5% and 2.7%, respectively, Fig. 2b2, c2, d2).

3.2. Root distributions

The total fine-root mass of *P. simonii* (344.3 g, the mean from the three cubes) in the 3.36 m^3 sampling cube (a total of 105 sub-cuboids) was much larger than the masses of the other three species: *C. korshinskii* (86.1 g), *S. psammophila* (113.0 g) and *A. ordosica* (60.1 g). The proportion of cumulative fine-root masses within 0-80 cm soil layer for *P. simonii*, *C. korshinskii*, *S. psammophila*, and *A. ordosica* accounted for 83%, 83%, 94%, 97%, respectively, of the total fine-root mass (Fig. 3). The differences in fine-root mass and distribution of fine-root in soil layers imply the various plants utilize somewhat different water sources.

3.3. Water sources and physiological characteristics

The simmr model results indicate the following (Fig. 4a) for the May to September period of the wet year (2018): (a) *P. simonii* mainly used water from deep layer (70-300 cm; mean of 41%), with less from shallow (0-30 cm; 24%) and intermediate (30-70 cm; 35%) layers; (b) *C. korshinskii* used more water from deep layer (39%) and similar fractions of shallow water (30%) and intermediate water (31%); (c) *S. psammophila* used more water from intermediate layer (38%) and similar fractions of shallow water (33%) and deep water (29%); and (d) *A. ordosica* generally relied on shallow soil water (57%), with limited use of water from intermediate (24%) and deep (19%) layers. The

309 utilization of shallow water by *P. simonii*, *C. korshinskii* and *S. psammophila* was
310 significantly lower than that of *A. ordosica*; and *P. simonii* had a significantly higher
311 utilization of deep soil water (bootstrapping test). During the dry year (2019), the
312 utilization of deep soil water increased relative to the wet year for all species (Fig. 4a):
313 *P. simonii* (54%), *C. korshinskii* (54%), *S. psammophila* (53%) and *A. ordosica* (37%).
314 The increases of *S. psammophila* and *A. ordosica* were significant (bootstrapping test).

315 The ranges of ψ_{md} values for the four species were quite different and
316 demonstrated yearly variability for *A. ordosica* (Fig. 4b). The ψ_{md} for *A. ordosica*
317 significantly decreased (bootstrapping test) from the wet year to the dry year,
318 suggesting that this sand-binding semi-shrub may manage water stress by stomatal
319 control. Regarding inter-species differences, *C. korshinskii* showed consistently lower
320 ψ_{md} (minimum value of -2.3MPa) than the other three species in both years
321 (bootstrapping test). In fact, it was the only species where the median ψ_{md} was higher
322 in the dry year than the wet year, although this response was not significant.

323 Foliar $\delta^{13}C$ for *C. korshinskii*, *S. psammophila* and *A. ordosica*, increased
324 significantly (became less negative) from the wet year to the dry year, whereas that for
325 *P. simonii* generally remained stable (bootstrapping test, Fig. 4c). *A. orodosia* showed
326 consistently lower $\delta^{13}C$ than the other three species; $\delta^{13}C$ for *C. korshinskii* and *S.*
327 *psammophila* were intermediate; and $\delta^{13}C$ for *P. simonii* was the highest recorded
328 among the four species in both years (bootstrapping test). These patterns imply
329 differentiation of physiological characteristics related to water use strategies between
330 species.

3.4. Hydrological Niche Separation

Based on the nicheROVER package, we find that in the wet year (Fig. 5, Table 2) *A. ordosica* individuals were largely absent from the niche regions of *P. simonii* (0% probability), *C. korshinskii* (3%), and *S. psammophila* (0%). These three species also had a relatively low probability of being found in the niche region of *A. ordosica*, suggesting HNS occurred between *A. ordosica* and the other three species. We also find an asymmetric overlap in isotope distributions between *P. simonii* and *C. korshinskii*. Further, *P. simonii* and *S. psammophila. P. simonii* had a high probability of utilizing water in niche regions of *C. korshinskii* and *S. psammophila* (68% and 45%, respectively), while *C. korshinskii* and *S. psammophila* had low probabilities of water use from the *P. simonii* niche region (20% and 18%, respectively). The probabilities of *S. psammophila* and *C. korshinskii* using water from each other´s niche regions were also high: 66% (*S. psammophila* in *C. korshinskii´*s niche region); and 60% (*C. korshinskii* in *S. psammophila´*s niche region).

In the dry year, the trends of HNS between species were consistent with those in the wet year but the degree of separation decreased slightly (Fig. 6, Table 3). *A. ordosica* individuals still had the lowest probability of water usage from the niche regions of *P. simonii* (4%), *C. korshinskii* (32%), and *S. psammophila* (16%). *P. simonii* individuals had the highest probability of water usage from the niche regions of *C. korshinskii* (84%) and *S. psammophila* (74%); the probabilities were lower for *C. korshinskii* (42%) and *S. psammophila* (32%).

4. Discussion

The four plants exhibited diverse water sources and physiological regulation strategies, resulting in different degrees of HNS between the species (Fig. 7). *P. simonii* relied on consistently deep soil water in both years – a result that is intuitive for an environment that dries from the surface downward during periods of low rainfall, guaranteeing high WUEi and stable ψ_{md}. The two shrubs similarly increased the use of deep soil water, and improved WUEi through stomatal regulation to cope with drought stress from the wet year to the dry year. Nevertheless, the response of ψ_{md} to these strategies was different. Both *C. korshinskii* and *S. psammophila* kept stable ψ_{md}. The ψ_{md} of the former was significantly lower than the latter, indicating that *S. psammophila* may have stricter stomatal control. This characteristic is in line with that reported by Zhao et al. (2021) regarding *S. psammophila* being an isohydric plant while *C. korshinskii* is an anisohydric plant. The regulation of stomata and the increase of WUEi and the contribution of deep soil water did not effectively curb the significant decrease of ψ_{md} for the semi-shrub *A. ordosica* from the wet year to the dry year. This finding was related to its shallow root depths and the limited ability to obtain deep water source compared with other three species.

The difference in WUEi and water sources within the soil profile resulted in HNS between *A. ordosica* and the other three species in the wet year. The hydrological niche overlap increased in the dry year as precipitation decreased. Collectively the differences in root water uptake depth and differentiations of physiological traits of coexisting species support the occurrence of HNS. Importantly, the shifts in water sources and

physiological characteristics from the wet year to the dry year indicate HNS is dynamic on at least an annual time scale in response to fluctuating soil moisture patterns, supporting our original hypothesis.

4.1. Water use strategies

The root distribution data and the simmr model outputs indicate different water-use strategies. For example, the tree (*P. simonii*) extracted proportionally more water from deeper layers than shallow layers in both wet and dry years, likely in association with the presence of its fine-root masses and overall root distributions. Within the 3.36 m^3 sampling cube, we observed a higher mass and proportion of fine roots in the deep layer for *P. simonii* compared with the other three species (note: we did not measure root mass changes from year to year). Therefore, *P. simonii* had a greater ability to obtain deep soil water than the three shrub species.

One shrub (*C. korshinskii*) relied on deep soil water, while the other shrub (*S. psammophila*) relied on intermediate soil water in the wet year, which is also supported by the root data showing that the proportion of fine-root at 80-140 cm soil layer for *C. korshinskii* (17%) is higher than that for *S. psammophila* (6%). As the semi-shrub *A. ordosica* had few fine roots deeper than 100 cm it mostly used water from the shallow soil in the wet year, which is generally expected.

Notably, water acquisition strategies for the four species shifted dynamically in response to moisture differences in the two years. All species increased their utilization of deep soil water and decreased their utilization of shallow water in the dry year that followed the wet year. Such a modification is considered an efficient strategy for

397 drought avoidance for most vegetation (Christina et al., 2017; Jiang et al., 2020; Yang
398 et al., 2017; Zhao et al., 2021).

399 Changes in soil water status not only resulted in shifts in the utilization of water
400 sources but they also affected the expression of plant physiological characteristics. The
401 similar ψ_{md} in both the wet and dry years does not support the notion that *P. simonii*
402 experienced significant water stress in the dry year, despite other research indicating
403 the lack of suitability for this species to cope with the dry conditions in CLP (Liang et
404 al., 2006; Wang et al., 2019). Compared with the other three species, *P. simonii* had the
405 highest foliar $\delta^{13}C$, which may be related to the high utilization of deep soil water. We
406 find a negative correlation between the contribution of shallow soil water and foliar
407 $\delta^{13}C$ (R^2=0.37, $p<0.001$; Fig. S3a), as well as a positive correlation between the
408 contribution of deep soil water and foliar $\delta^{13}C$ (R^2=0.38, $p<0.001$; Fig. S3c).
409 Unfortunately, our limited number of samples does not allow us to explore this
410 relationship in more detail for individual species.

411 ψ_{md} for the two shrubs (*C. korshinskii* and *S. psammophila*) remained stable during
412 both years, but their foliar $\delta^{13}C$ increased significantly, a trait that may allow them to
413 cope against water stress. A decline in water availability causes plants to close their
414 stomata and decrease their discrimination against ^{13}C during photosynthesis, resulting
415 in higher $\delta^{13}C$ values and increased water-use efficiency (Camarero et al., 2018;
416 Francey & Farquhar, 1982). Similarly, the $\delta^{13}C$ values in *A. ordosica* increased during
417 the dry year. However, its ψ_{md} decreased significantly, indicating substantial water
418 stress, probably because of its inability to access more deep soil water owing to limited

root mass.

4.2. Dynamic Hydrological Niche Segregation

The magnitude of the observed HNS varied with water availability, indicating that the hydrological niches were dynamic. The hydrological niche of *A. ordosica* was clearly separated from those of the other three species in the wet year when there was a very low probability (0-3%) of it using water from the hydrological niches of the other species. However, that probability increased to 4-32% in the dry period, reducing the degree of separation (Table 2). In general, the probability of overlap in hydrological niches among all species increased during the dry year, with the exception being the overlap between *S. psammophila* and *C. korshinskii*. In most cases, the HNS was highest in the wet year.

A decrease in the HNS and an increase in competition for water among the four species in arid ecosystems can be expected as precipitation decreases. The four plants utilized diverse water sources in the wet year, while in the dry year, they used deeper soil water more frequently (Fig. 7). The higher usage of deep soil water in the dry year resulted in a higher overlap in their hydrological niches. Similar trends were observed in the Taihang Mountains of China, where *Vitex negundo* L. var. heterophylla had a high hydrological niche overlap with *Robinia pseudoacacia* L and *Ziziphus jujuba* Mill var. spinosa during the dry season (Zhu et al., 2021). However, during the rainy season, these species had a greater HNS.

Nevertheless, we need to clarify that HNS relates to differences in root water uptake depths as well as differentiation of physiological traits. The assessment of HNS

in our study was based on comparisons of isotopes in the xylem water and the water within the soil profile, as well as WUEi (foliar $\delta^{13}C$). Thus, the magnitude of HNS does not depend entirely on the shift in plant water sources. For example, although *A. ordosica* utilized the water throughout the soil profile, its main water source differed from the other three species in the wet year, implying that there could be weak water competition between them.

The hydrological niche overlap between *A. ordosica* and the other three species ranged from 6 to 22%, using $\delta^{2}H$ and $\delta^{18}O$ (Table S1), which aligns with the expected results of lower water competition. However, the values ranged from 0 to 3%, using $\delta^{2}H$, $\delta^{18}O$ and $\delta^{13}C$, suggesting that the hydrological niche of *A. ordosica* was clearly separated from those of the other three species. We surmise that, in addition to difference in water sources, differentiation in physiological traits between *A. ordosica* and the other three species contributes to a higher HNS between them. The difference in physiological regulation between species is also indicated by the lower $\delta^{13}C$ in *A. ordosica* than in the other three species in the wet year.

It has been widely recognized that species adopt different root water use depths and physiological regulations in response to drought stress and/or water competition (Araya et al., 2011; Brum et al., 2019; Dwyer et al., 2021; Granda et al., 2022; Palacio et al., 2017). Discussion above in 4.1 similarly suggests differences in water use strategies of the four species. Thus, a single consideration of water acquisition for species may not systematically indicate how plants respond to water competition. In this context, our study is the first to assess the HNS under the dual control of water

acquisition via roots and water loss through stomata. These comparisons allow for a more complete understanding of the water relationship between species.

4.3. Limitations and future considerations

Our research adds to the understanding of dynamic HNS, but we acknowledge that our methods may not have captured the full range of hydrological niche widths. We only compared overlap between species in two years, using plant samples from May to September 2018 and 2019, which correspond with wet and dry years, respectively. While we collected data for five months, a longer time frame may have shown more seasonal variation and a broader hydrological niche. In our study area, most of the precipitation occurred from July to September, with May to June being relatively dry. This uneven annual precipitation distribution led to large differences in the dual space of $\delta^{18}O/\delta^{2}H$ and $\delta^{13}C$ values in the wet year (2018) for *A. ordosica*, as seen in the two isotope clusters in Figs. 5g-h. In this case, it seems that using a single ellipsoid obtained by nicheROVER to fit these two segmented isotope clusters may not be ideal as it may influence the estimation of niche region and overlap. Additionally, data from an additional very dry year would have allowed us to assess the water stress of all plants and potentially greater HNS.

Recently, the use of cryogenic vacuum distillation techniques in hydrogen isotopic fractionation has been questioned as a possible cause of conflicting results in various studies (Chen et al., 2020). While some research supports this view (e.g., Millar et al., 2019), other studies provide evidence to the contrary (Allen & Kirchner, 2022; Amin et al., 2021; Evaristo et al., 2021; Newberry et al., 2017). Evaristo et al. (2017) found that

using both δ^2H and $\delta^{18}O$ in a Bayesian inference framework improved estimates of plant water sources. Therefore, we used both δ^2H and $\delta^{18}O$ to evaluate plant water sources and combined them with $\delta^{13}C$ values to measure HNS among species. While the results are plausible, we cannot confidently say that combining stable isotope tracers with the nicheROVER model fully captures the extent of hydrological niches. More data is needed from a variety of wetness conditions and other species.

Our approach also only allowed us to estimate the proportions of water use from three soil layers, but not the volumes of water use. This information would have been useful in understanding how plants in the community manage water stress in general. It would also have been helpful to track changes in root mass and distribution over time to better interpret our findings. Additionally, we only considered water as a limiting factor on community structure, but light and nutrient availability also play important roles in vegetation dynamics (Brum et al., 2019; Stark et al., 2012, 2015). Future research should focus on quantifying the potential trade-offs between plant water uptake and light availability at the community level and modeling water dynamics at the rhizosphere scale (Daly et al., 2017).

5. Conclusion

Our results indicate that the four coexisting plant species (*P. simonii*, *C. korshinskii*, *S. psammophila* and *A. ordosica*) in this dry ecosystem segregate along a hydrological niche axis defined by water sources and WUEi, which is reflected in their xylem water isotopes (δ^2H and $\delta^{18}O$) and foliar $\delta^{13}C$. The extent of HNS among species decreased

from the wet year to the dry year because of changes in access to water sources and WUEi. *P. simonii* readily used water in the deeper soil layers during both wet and dry years, meanwhile WUEi remained stable. While three of the shrub and semi-shrub species (*C. korshinskii*, *S. psammophila* and *A. ordosica*) not only increased the deep soil water use in the dry year, they also increased WUEi through stomatal regulation, leading to greater competition for water in the dry year versus the wet year. This study shows that in dry ecosystems, HNS changes throughout the year as plant adjust water resource acquisition and alter WUEi in response to variable soil moisture levels. A better understanding of the dynamics of HNS of coexisting species will help researchers to make more informed predictions about future changes in the abundance and structure of plant communities in arid and semi-arid regions in response to climatic variability and forecasted climate changes.

Acknowledgements

We thank Prof. Martin Wassen and Prof. Stefan Dekker of the Copernicus Institute of Sustainable Development, Faculty of Geosciences, for making the research visit of Ying Zhao to Utrecht University possible. This work was supported by the National Natural Science Foundation of China (41771545; 41977012), the Strategic Priority Research Program of Chinese Academy of Sciences (XDB40000000) and the State Key Laboratory of Loess and Quaternary Geology, Institute of Earth Environment, CAS (SKLLQG1718).

Author contributions

The experiment was designed and planned by YZ, LW and JE. The field work and sample collection were performed by YZ and LW. Data were analyzed and the manuscript was drafted by YZ and ADZ with assistance from JE, KPC and LW. All authors contributed to the final manuscript.

Competing interests

The authors have no conflicts of interest to declare.

Data availability

The data that support the findings of this study are available from the corresponding author upon reasonable request.

References

Allen, S.T., Kirchner, J.W. 2022. Potential effects of cryogenic extraction biases on plant water source partitioning inferred from xylem-water isotope ratios. Hydrological Processes, 36, e14483.

Amin, A., Zuecco, G., Marchina, C., Engel, M., Penna, D., McDonnell, J. J., Borga, M. 2021. No evidence of isotopic fractionation in olive trees (*Olea europaea*): a stable isotope tracing experiment. Hydrological Sciences Journal, 66(16), 2415-2430.

Araya, Y.N., Silvertown, J., Gowing, D.J., McConway, K.J., Linder, H.P., Midgley, G.

2011. A fundamental, eco-hydrological basis for niche segregation in plant communities. New Phytologist, 189, 253-258.

Armas, C., Pugnaire, F.I. 2005. Plant interactions govern population dynamics in a semi-arid plant community. Journal of Ecology, 93, 978-989.

Bartelheimer, M., Gowing, D.J., Silvertown, J. 2010. Explaining hydrological niches: the decisive role of below-ground competition in two closely related Senecio species. Journal of Ecology, 98, 126-136.

Brum, M., Vadeboncoeur, M.A., Ivanov, V., Asbjornsen, H., Saleska, S., Alves, L.F., Penha, D., et al. 2019. Hydrological niche segregation defines forest structure and drought tolerance strategies in a seasonal Amazon forest. Journal of Ecology, 107, 318-333.

Camarero, J.J., Sanchez-Salguero, R., Sanguesa-Sarreda, G., Matias, L. 2018. Tree species from contrasting hydrological niches show divergent growth and water-use efficiency. Dendrochronologia, 52, 87-95.

Cao, S.X. 2008. Why large-scale afforestation efforts in China have failed to solve the desertification problem. Environmental Science & Technology, 42(6), 1826-1831.

Cao, S.X., Chen, L., Shankman, D., Wang, C.M., Wang, X.B., Zhang, H. 2011. Excessive reliance on afforestation in China's arid and semi-arid regions: Lessons in ecological restoration. Earth-Science Reviews, 104, 240-245.

Cao, S.X., Tian, T., Chen, L., Dong, X.B., Yu, X.X., Wang, G.S. 2010. Damage caused to the environment by reforestation policies in arid and semi-Arid areas of China. AMBIO, 39, 279-283.

Case, M.F., Nippert, J.B., Holdo, R.M., Staver, A.C. 2020. Root-niche separation between savanna trees and grasses is greater on sandier soils. Journal of Ecology, 00, 1-11.

Chen, Y.L., Helliker, B.R., Tang, X., Li, F., Zhou, Y., Song, X. 2020. Stem water cryogenic extraction biases estimation in deuterium isotope composition of plant source water. Proceedings of the National Academy of Sciences, 117, 33345-33350.

Chen, Y., Wang, K., Lin, Y., Shi, W., Song, Y., He, X. 2015. Balancing green and grain trade. Nature Geoscience, 8, 739-741.

Christina, M., Nouvellon, Y., Laclau, J-P, Stape, J.L., Bouillet, J-P., Lambais, G.R., le Maire, G. 2017. Importance of deep water uptake in tropical eucalypt forest. Functional Ecology, 31, 509-519.

Dai, J.J., Zhang, X.P., Luo, Z.D., Wang, R., Liu, Z.L., He, X.G., Rao, Z.G., et al. 2020. Variation of the stable isotopes of water in the soil-plant-atmosphere continuum of a Cinnamomum camphora woodland in the East Asian monsoon region. Journal of Hydrology, 589, 125199.

Daly, K.R., Cooper, L.J., Koebernick, N., Evaristo, J., Keyes, S.D., van Veelen, A., Roose, T. 2017. Modelling water dynamics in the rhizosphere. Rhizosphere, 4, 139-151.

Dwivedi, A. K., Mallawaarachchi, I.,, Alvarado, L. A. 2017. Analysis of small sample size studies using nonparametric bootstrap test with pooled resampling method. Statistics in medicine, 36(14), 2187-2205.

Dwyer, C., Pakeman, R.J., Jones, L., van Willegen, L., Hunt, N., Millett, J. 2021. Fine-scale hydrological niche segregation in coastal dune slacks. Journal of Vegetation Science, 32, e13085.

Evaristo, J., Jameel, Y., Chun, K.P. 2021. Implication of stem water cryogenic extraction experiment for an earlier study is not supported with robust context-specific statistical assessment. Proceedings of the National Academy of Sciences, 118(17), e2100365118.

Evaristo, J., McDonnell, J.J., Clemens, J. 2017. Plant source water apportionment using stable isotopes: a comparison of simple linear, two-compartment mixing model approaches. Hydrological Processes, 31, 3750-3758.

Evaristo, J., McDonnell, J.J., Scholl, M.A., Bruijnzeel, L.A., Chun, K.P. 2016. Insights into plant water uptake from xylem-water isotope measurements in two tropical catchments with contrasting moisture conditions. Hydrological Processes, 30, 3210-3227.

Francey, R.J., Farquhar, G.D. 1982. An explanation of $^{13}C/^{12}C$ variations in tree rings. Nature, 297, 28-31.

Fu, B.J., Wang, S., Liu, Y., Liu, J.B., Liang, W., Miaom C.Y. 2017. Hydrogeomorphic ecosystem responses to natural and anthropogenic changes in the Loess Plateau of China. Annual Review of Earth and Planetary Sciences, 45, 223-243.

Granda, E., Antunes, C., Máguas, C., Castro- Díez, P. 2022. Water use partitioning of native and non- native tree species in riparian ecosystems under contrasting climatic conditions. Functional Ecology, 36, 2480-2492.

Guderle, M., Bachmann, D., Milcu, A., Gockele, A., Bechmann, M., Fischer, C., Roscher, C., et al. 2018. Dynamic niche partitioning in root water uptake facilitates efficient water use in more diverse grassland plant communities. Functional Ecology, 32, 214-227.

Hesterberg, T. 2011. Bootstrap. Wiley Interdisciplinary Reviews: Computational Statistics, 3(6), 497-526.

Holdo, R.M., Nippert, J.B. 2022. Linking resource- and disturbance- based models to explain tree-grass coexistence in savannas. New Phytologist.

Ivanov, V.Y., Hutyra, L.R., Wofsy, S.C., Munger, J.W., Saleska, S.R., de Oliveira Jr, R.C., de Camargom P.B. 2012. Root niche separation can explain avoidance of seasonal drought stress and vulnerability of overstory trees to extended drought in a mature Amazonian forest, Water Resources Research, 48, W12507.

Jackson, A.L., Inger,R., Parnell, A.C., Bearhop, S. 2011. Comparing isotopic niche widths among and within communities: SIBER-Stable Isotope Bayesian Ellipses in R. Journal of Animal Ecology, 80, 595-602.

Jiang, P., Wang, H., Meinzer, F.C., Kou, L., Dai, X., Fu, X. 2020. Linking reliance on deep soil water to resource economy strategies and abundance among coexisting understorey shrub species in subtropical pine plantations. New Phytologist, 225, 222-233.

Kang, Y.X., Kang, B.W., Yue, W.J., Liang, Z.S., Lei, R.D. 2007. The classification of Quercus liaotungensis communities and their nich in Loess Plateau of North Shaanxi. Acta Ecologica Sinica, 27, 4096-4105 (in Chinese with English abstract)

Kulmatiski, A., Adler, P.B., Foley, K.M. 2020b. Hydrologic niches explain species coexistence and abundance in a shrub-steppe system. Journal of Ecology, 108, 998-1008.

Kulmatiski, A., Beard, K.H., Holdrege, M.C., February, E.C. 2020a. Small differences in root distributions allow resource niche partitioning. Ecology and Evolution, 10, 9776-9787.

Kulmatiski, A., Beard, K.H. 2022. A modern two-layer hypothesis helps resolve the 'savanna problem'. Ecology Letters, 25(9), 1952-1960.

Liang, Z.S., Yang, J.W., Shao, H.B., Han, R.L. 2006. Investigation on water consumption characteristics and water use efficiency of poplar under soil water deficits on the Loess Plateau. Colloids and Surfaces B: Biointerfaces, 53, 23-28.

Liu, T.S. 1985. Loess and the environment. (China's) Science Press, Beijing (in Chinese)

Lu, F., Hu, H.F., Sun, W.J., Zhu, J.J., Liu, G.B., Zhou, W.M., Zhang, Q.F., et al. 2018. Effects of national ecological restoration projects on carbon sequestration in China from 2001 to 2010. Proceedings of the National Academy of Sciences of the United States of America, 115(16), 4039-4044.

Matos, I. S., Binks, O., Eller, C. B., Zorger, B. B., Meir, P., Dawson, T. E.,, Rosado, B. H. 2022. Revisiting plant hydrological niches: The importance of atmospheric resources for ground-rooted plants. Journal of Ecology, 110(8), 1746-1756.

Millar, C., Pratt, D., Schneider, D., Koehler, G., McDonnell, J.J. 2019. Further experiment comparing direct vapor equilibration and cryogenic vacuum distillation for plant water stable isotope analysis. Rapid Communications in Mass

Spectrometry, 33, 1850-1854.

Moreno-Gutierrez, C., Dawson, T.E., Nicolas, E., Querejeta, J.I. 2012. Isotopes reveal contrasting water use strategies among coexisting plant species in a Mediterranean ecosystem. New Phytologist, 196(2), 489-496.

Newberry, S.L., Nelson, D.B., Kahmen, A. 2017. Cryogenic vacuum artifacts do not affect plant water-uptake studies using stable isotope analysis. Ecohydrology, 10, e1892.

Palacio, S., Montserrat-Marti, G., Ferrio, J.P. 2017. Water use segregation among plants with contrasting root depth and distribution along gypsum hills. Journal of Vegetation Science, 28, 1107-1117.

Parnell, A.C., Phillips, D.L., Bearhop, S., Semmens, B.X., Ward, E.J., Moore, J.W., Jackson, A.L., et al. 2013. Bayesian stable isotope mixing models. Environmetrics, 24 (6), 387-399.

Rodríguez-Robles, U., Arredondo, J.T., Huber-Sannwald, E., Yepez, E.A., Ramos-Leal, J.A. 2020. Coupled plant traits adapted to wetting/drying cycles of substrates co-define niche multidimensionality. Plant Cell & Environment, 43, 2394-2408.

Seibt, U., Rajabi, A., Griffiths, H., Berry, J. A. 2008. Carbon isotopes and water use efficiency: sense and sensitivity. Oecologia, 155(3), 441-454.

Silvertown, J., Araya, Y., Gowing, D. 2015. Hydrological niches in terrestrial plant communities: a review. Journal of Ecology, 103, 93-108.

Stark, S.C., Enquist, B.J., Saleska, S.R., Leitold, V., Schietti, J., Longo, M., Alves, L.F., et al. 2015. Linking canopy leaf area and light environments with tree size

distributions to explain Amazon forest demography. Ecology Letters, 18, 636-645.

Stark, S.C., Leitold, V., Wu, J.L., Hunter, M.O., de Castilho, C.V., Costa, F.R.C., McMahon, S.M., et al. 2012. Amazon forest carbon dynamics predicted by profiles of canopy leaf area and light environment. Ecology Letters, 15, 1406-1414.

Swanson, H., Lysy, M., Ehrman-Stasko, A., Johnson, J., Reist, J. 2015. A new probabilistic method for quantifying *n*-dimensional ecological niches and niche overlap. Ecology, 96, 318-324.

Tsunekawa A, Liu G, Yamanaka N, Du S, eds. 2014. Restoration and development of the degraded Loess Plateau. Tokyo: Springer Japan.

Walter, H. 1939. Grasland, Savanne und Busch der arideren Teile Afrikas in ihrer ökologischen Bedingtheit. Jahrb Wiss Bot, 87,750-860.

Wang, S., Fan, J., Ge, J.M., Wang, Q.M., Fu, W. 2019. Discrepancy in tree transpiration of *Salix matsudana*, *Populus simonii* under distinct soil, topography conditions in an ecological rehabilitation area on the Northern Loess Plateau. Forest Ecology and Management, 432, 675-685.

Ward, D., Wiegand, K., Getzin, S. 2013. Walter's two-layer hypothesis revisited: Back to the roots! Oecologia, 172, 617-630.

Wu, J.E., Zeng, H.H., Zhao, F., Chen, C.F., Singh, A.K., Jiang, X.J., Yang, B., Liu, W.J. 2022. Plant hydrological niches become narrow but stable as the complexity of interspecific competition increases. Agricultural and Forest Meteorology, 320, 108953.

Yang, F.T., Feng, Z.M., Wang, H.M., Dai, X.Q., Fu, X.L. 2017. Deep soil water

extraction helps to drought avoidance but shallow soil water uptake during dry season controls the inter-annual variation in tree growth in four subtropical plantations. Agricultural and Forest Meteorology, 234-235, 106-114.

Yuan, C., Gao, G.Y., Fu, B.J. 2017. Comparisons of stemflow and its bio-abiotic influential factors between two xerophytic shrub species. Hydrology and Earth System Sciences, 21, 1421-1438.

Zhang, P.C., Wang, B.K., Tang, K.L. 1993. The environmental geomorphology characteristics of Shenmu experimental area. Memoir of NISWC, Academia Sinica and Ministry of Water Resources, 18, 16-23 (in Chinese with English abstract).

Zhao, Y., Wang, L., Knighton, J., Evaristo, J., Wassen, M. 2021. Contrasting adaptive strategies by *Caragana korshinskii* and *Salix psammophila* in a semiarid revegetated ecosystem. Agricultural and Forest Meteorology, 300, 108323.

Zhao, Y., Dai, J.J., Tang, Y.K., Wang, L. 2022. Illuminating isotopic offset between bulk soil water and xylem water under different soil water conditions. Agricultural and Forest Meteorology, 325, 109150.

Zhu, W.R., Li, W.H., Shi, P.L., Cao, J.S., Zong, N., Geng, S.B. 2021. Intensified interspecific competition for water after afforestation with *Robinia pseudoacacia* into a native shrubland in the Taihang Mountains, Northern China. Sustainability, 13, 807.

Figures

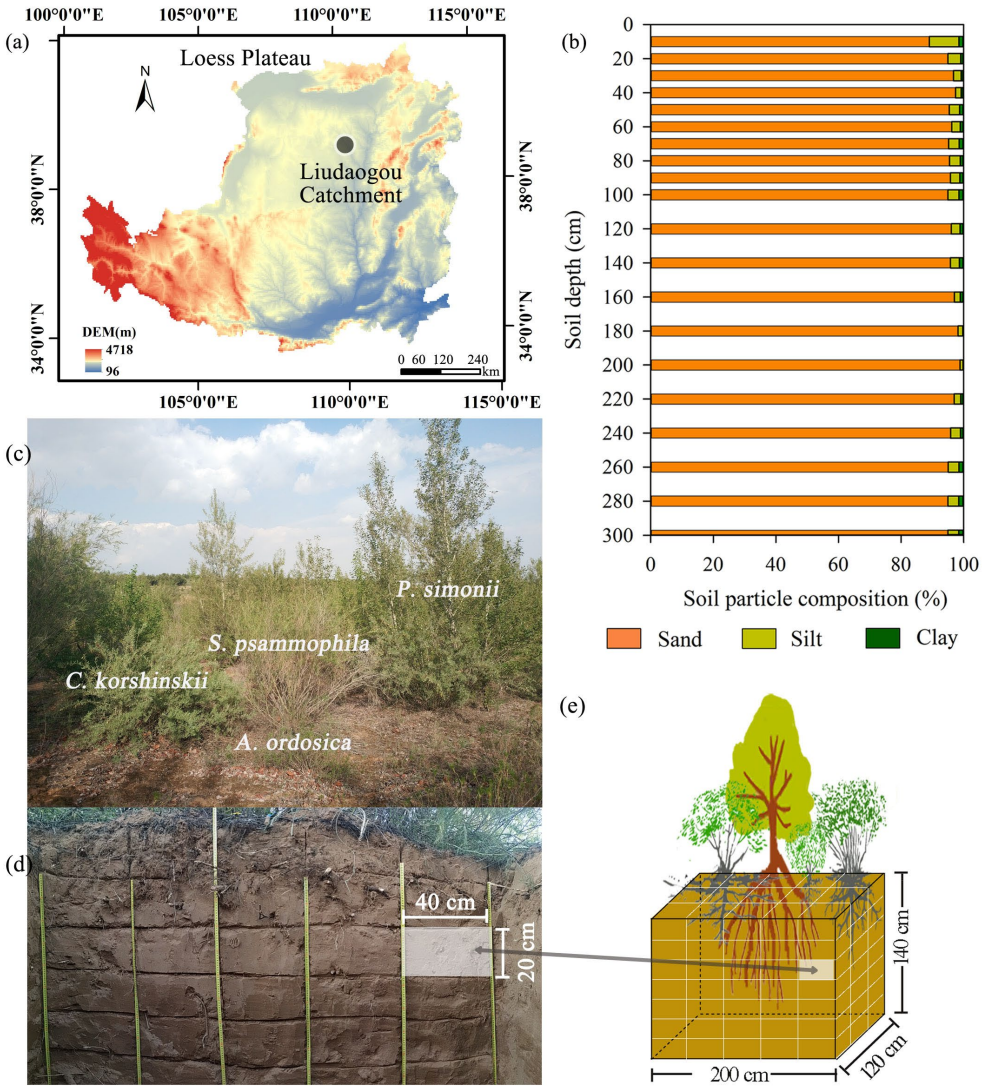

Fig. 1 Geographical location of the study area (a). Soil particle composition at 0-300 cm depths (b), photographs of four coexisting plant species (*P. simonii, S. psammophila, C. korshinskii* and *A. ordosica*) (c), and root excavations (not all depths are shown for clarity, d), and schematic of root excavations from one cuboid in one direction in our study area (e).

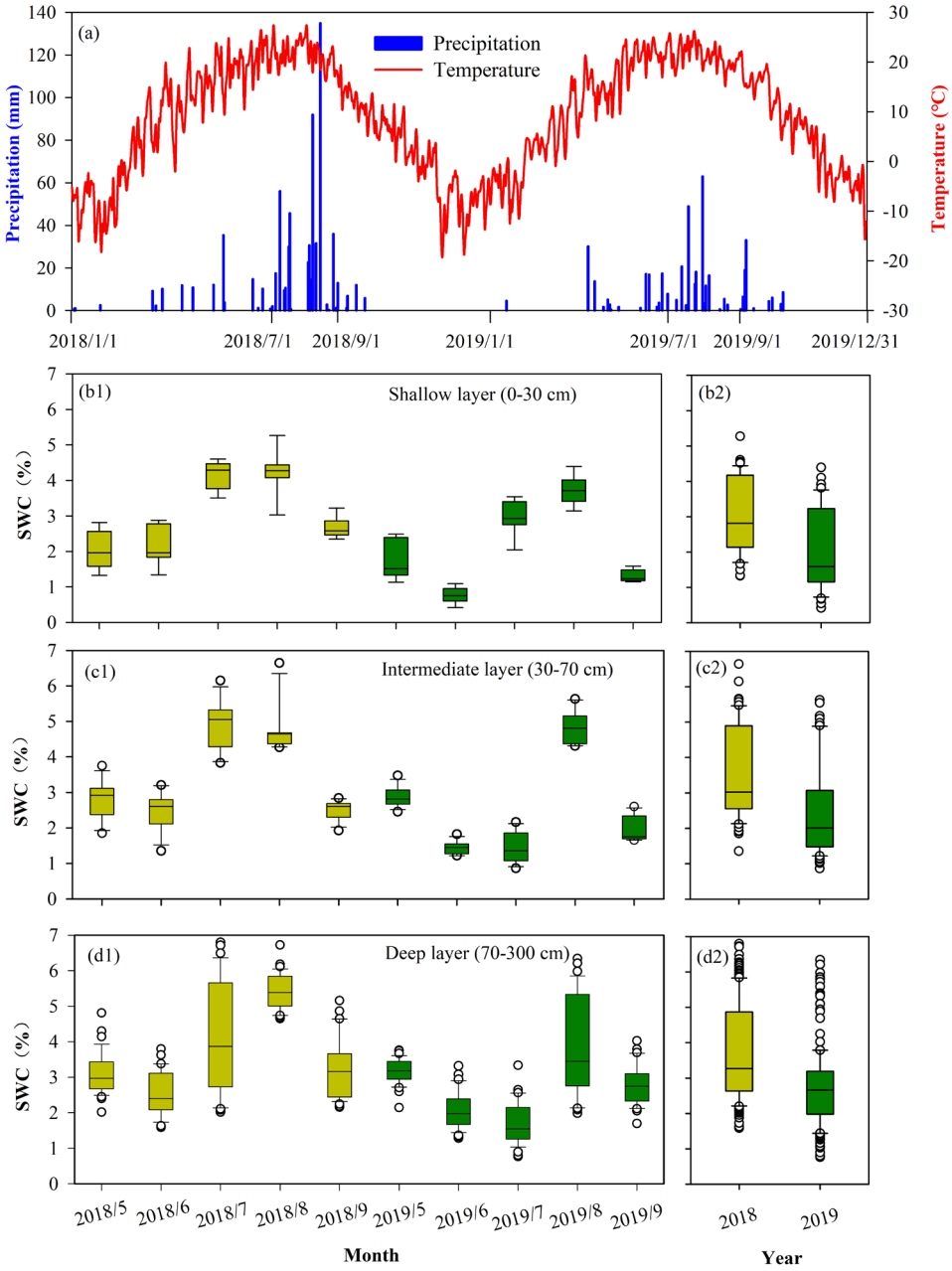

Fig. 2 Daily time series of precipitation and temperature (a), and boxplots of monthly and yearly variations in gravimetric soil water content (SWC) at shallow layer (b1-2, N=9 per month), intermediate layer (c1-2, N=12 per month) and deep layer (d1-2, N=39 per month) for 2018 in olive green and 2019 in dark green. Boxplots show the median (horizontal line), first to third quartiles (box), maximum and minimum values (whiskers) and outliers (points).

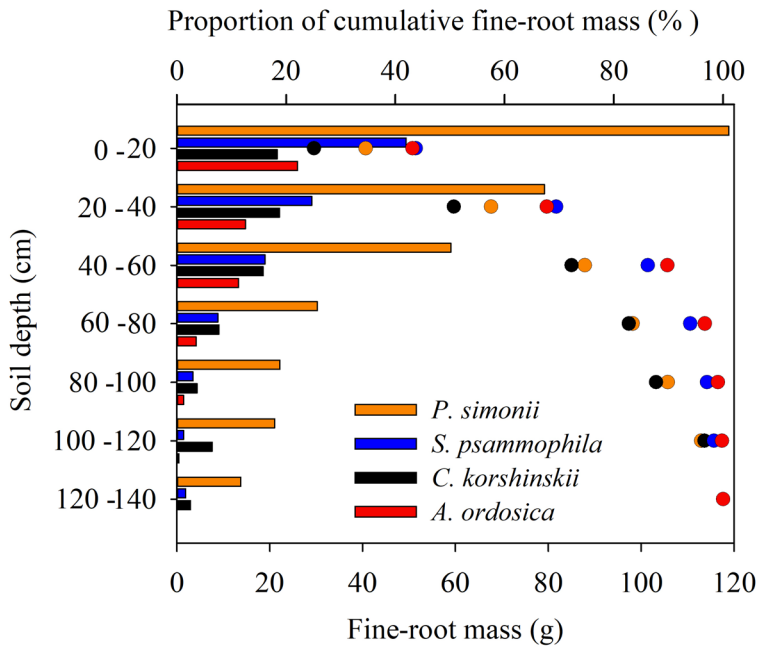

Fig. 3 Distributions of fine-root mass (bar) and the proportion of cumulative fine-root masses (scatter point) of *P. simonii*, *C. korshinskii*, *S. psammophila* and *A. ordosica*.

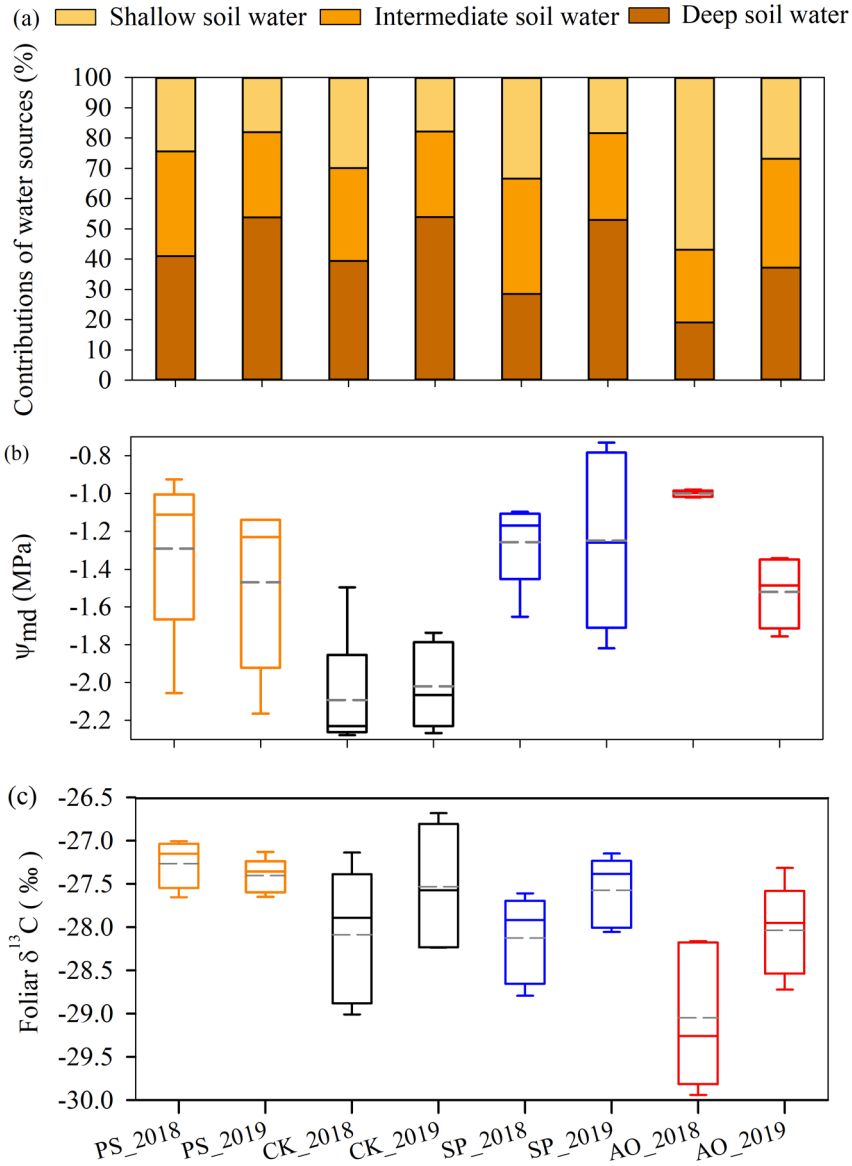

Fig. 4 Contributions of potential water sources (a), boxplots of ψ_{md} (b) and foliar $\delta^{13}C$ (c) for PS (*P. simonii*), CK (*C. korshinskii*), SP (*S. psammophila*) and AO (*A. ordosica*) in the wet (2018) and dry (2019) years. Boxplots show the median (horizontal solid line), mean (horizontal grey dash line), first to third quartiles (box), maximum and minimum values (whiskers). Data was collected monthly from May to September, 2018-2019 (N=5 for each boxplot).

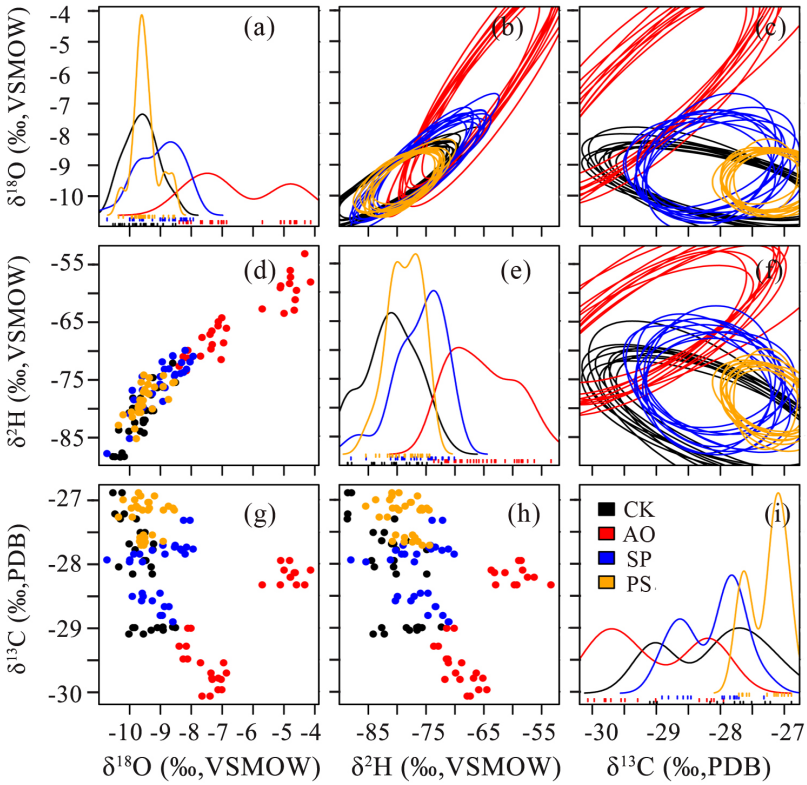

Fig. 5 Density distributions (probability of the random variable to fall within the range of observed values; a, $\delta^{18}O$; e, $\delta^{2}H$; i, $\delta^{13}C$), hydrological niche overlap plots (ten random elliptical projections of niche region for each species; b-c, f), and scatterplots (d, g-h) of four species (black, CK, *C. korshinskii*; red, AO, *A.ordosica*; blue, SP, *S.psammophila*; yellow, PS, *P. simonii*, N=30 per species) in the wet year (2018). Ten random elliptical projections of niche region were obtained by drawing 10 random pairs (mean, variance) for each species from their posterior distribution (Fig. S2a). The larger the ellipse overlap area between the two species, the higher the hydrological niche overlap.

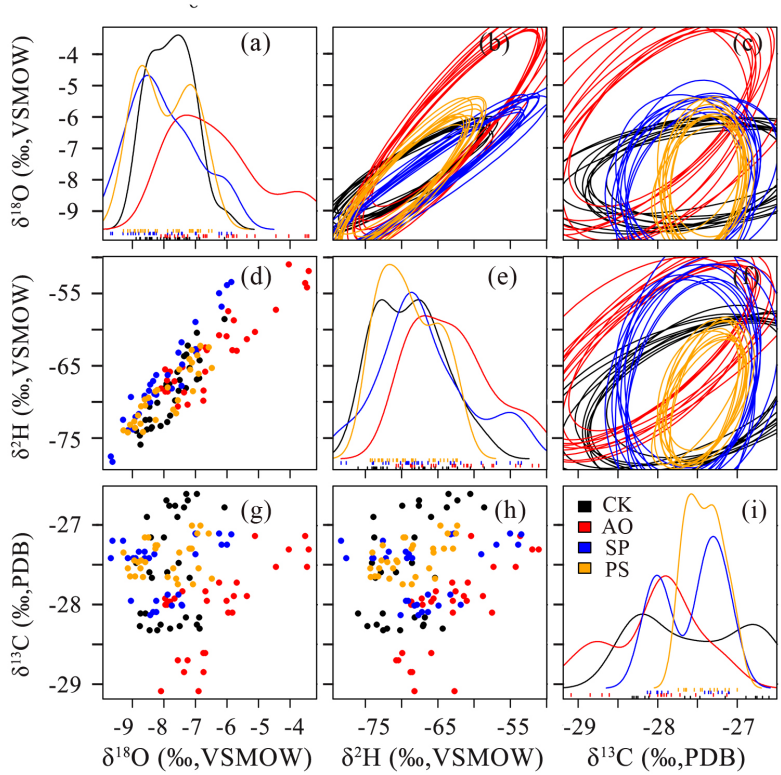

Fig. 6 Density distributions (probability of the random variable to fall within the range of observed values; a, $\delta^{18}O$; e, $\delta^{2}H$; i, $\delta^{13}C$), isotopic niche overlap plots (ten random elliptical projections of niche region for each species; b-c, f), and scatterplots (d, g-h) of four species (black, CK, *C. korshinskii*; red, AO, *A.ordosica*; blue, SP, *S.psammophila*; yellow, PS, *P. simonii*, N=30 per species) in the dry year (2019). Ten random elliptical projections of niche region were obtained by drawing 10 random pairs (mean, variance) for each species from their posterior distribution (Fig. S2b). The larger the ellipse overlap area between the two species, the higher the hydrological niche overlap.

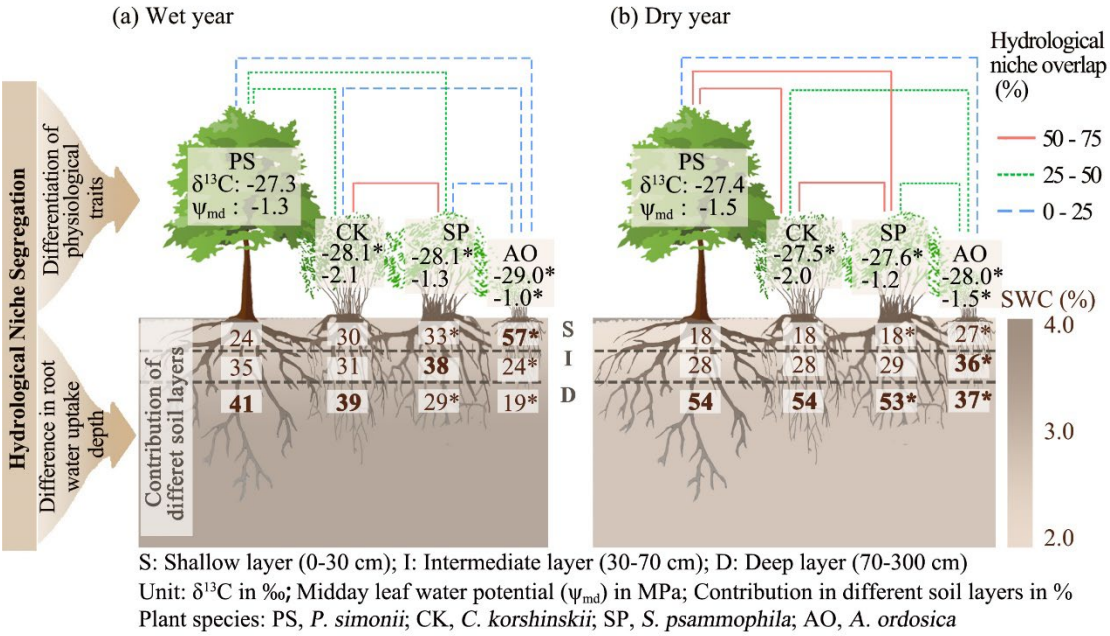

S: Shallow layer (0-30 cm); I: Intermediate layer (30-70 cm); D: Deep layer (70-300 cm)
Unit: $\delta^{13}C$ in ‰; Midday leaf water potential (ψ_{md}) in MPa; Contribution in different soil layers in %
Plant species: PS, *P. simonii*; CK, *C. korshinskii*; SP, *S. psammophila*; AO, *A. ordosica*

Fig. 7 Graphical summary of yearly changes in contributions of different soil layers, $\delta^{13}C$, ψ_{md}, and hydrological niche overlap of the four coexisting species. Asterisks indicate significant differences in water source, $\delta^{13}C$ and ψ_{md} for each species between the wet and the dry years. Hydrological niche overlap is the mean of species A versus species B and B versus A. The bold text in the soil profile indicates the water source that the species mainly relies on.

Tables

Table 1 Morphological parameters (mean ±1 s.d.) of the four plant species measured in the ecological sample survey.

	P. simonii	*C. korshinskii*	*S. psammophila*	*A. ordosica*
Growth form	Tree	Shrub	Shrub	Semi-shrub
Family	Salicaceae	Leguminosae	Salicaceae	Compositae
Leaf phenology	Deciduous	Deciduous	Deciduous	Deciduous
Average height in plots (m)	5.2±1.6	1.4±0.4	1.4±0.4	0.5±0.2
Average height of sampled plants (m)	5.2±0.8	1.3±0.4	1.4±0.4	0.6±0.3
Average basal diameter in plots (cm)	9.1±5.9	1.6±0.6	1.8±0.5	0.8±0.7
Average basal diameter of sampled plants (cm)	9.5±1.0	1.5±0.5	1.7±0.5	0.9±0.7
Density (individuals/ha)	519	494	301	3356
Root density (shallow, g m^{-3})	247.7	45.0	102.9	54.0
Root density (intermediate, g m^{-3})	144.0	42.3	50.0	29.2
Root density (deep, g m^{-3})	45.4	12.4	8.1	3.2
Number of plants in plots	187	64	39	435

Table 2 Mean probabilistic niche overlap (%) among the four plant species in the wet year (2018).

	A. ordosica	*C. korshinskii*	*P. simonii*	*S. psammophila*
A. ordosica	NA	3	0	0
C. korshinskii	4	NA	20	60
P. simonii	0	68	NA	45
S. psammophila	1	66	18	NA

Note: the numbers indicate the probability that an individual from the species indicated by the row will be found within the niche of the species indicated by the column header.

Table 3 Mean probabilistic niche overlap (%) among the four plant species in the dry year (2019).

	A. ordosica	*C. korshinskii*	*P. simonii*	*S. psammophila*
A. ordosica	NA	32	4	16
C. korshinskii	42	NA	42	51
P. simonii	29	84	NA	74
S. psammophila	42	49	32	NA

Note: the numbers indicate the probability that an individual from the species indicated by the row will be found within the niche of the species indicated by the column header.

Supplementary material for

Dynamic hydrological niche segregation: how plants compete for water in a semiarid ecosystem

Ying Zhao[1,2,5], Li Wang[1,2*], Kwok P. Chun[3], Alan D. Ziegler[4], Jaivime Evaristo[5*]

[1]State Key Laboratory of Soil Erosion and Dryland Farming on the Loess Plateau, Institute of Soil and Water Conservation, Northwest A&F University, Yangling, Shaanxi, China

[2]Institute of Soil and Water Conservation, Chinese Academy of Sciences and the Ministry of Water Resources, Yangling, Shaanxi, China

[3]Department of Geography and Environmental Management, University of the West of England, Bristol, UK

[4]Faculty of Fishery Technology and Aquatic Resources, Mae Jo University, Chiang Mai, Thailand

[5]Copernicus Institute of Sustainable Development, Utrecht University, Utrecht, the Netherlands

Contents of this file:

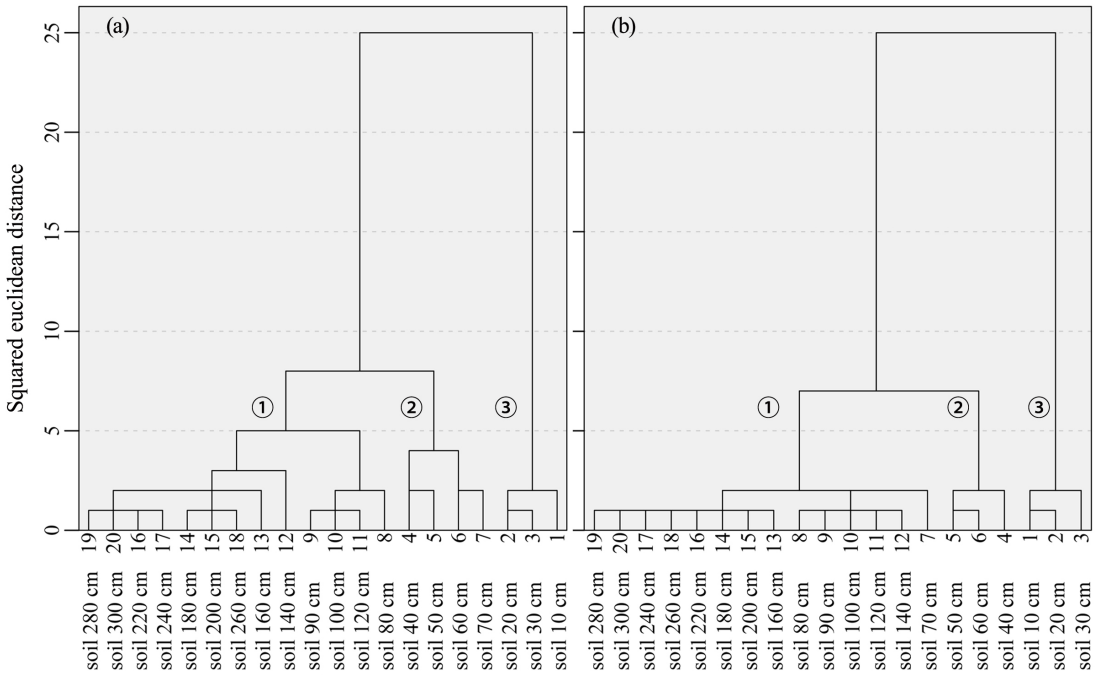

Fig. S1 Soil cluster analysis using 0-300 cm soil water $\delta^{18}O$ values (a) and $\delta^{2}H$ values (b), respectively, in 2018-2019. The numbers ① - ③ represented that soil water was divided into 3 groups, 0-30 cm, 30-70 cm and 70-300 cm using $\delta^{18}O$ values, and 0-30 cm, 30-60 cm and 60-300 cm using $\delta^{2}H$ values.

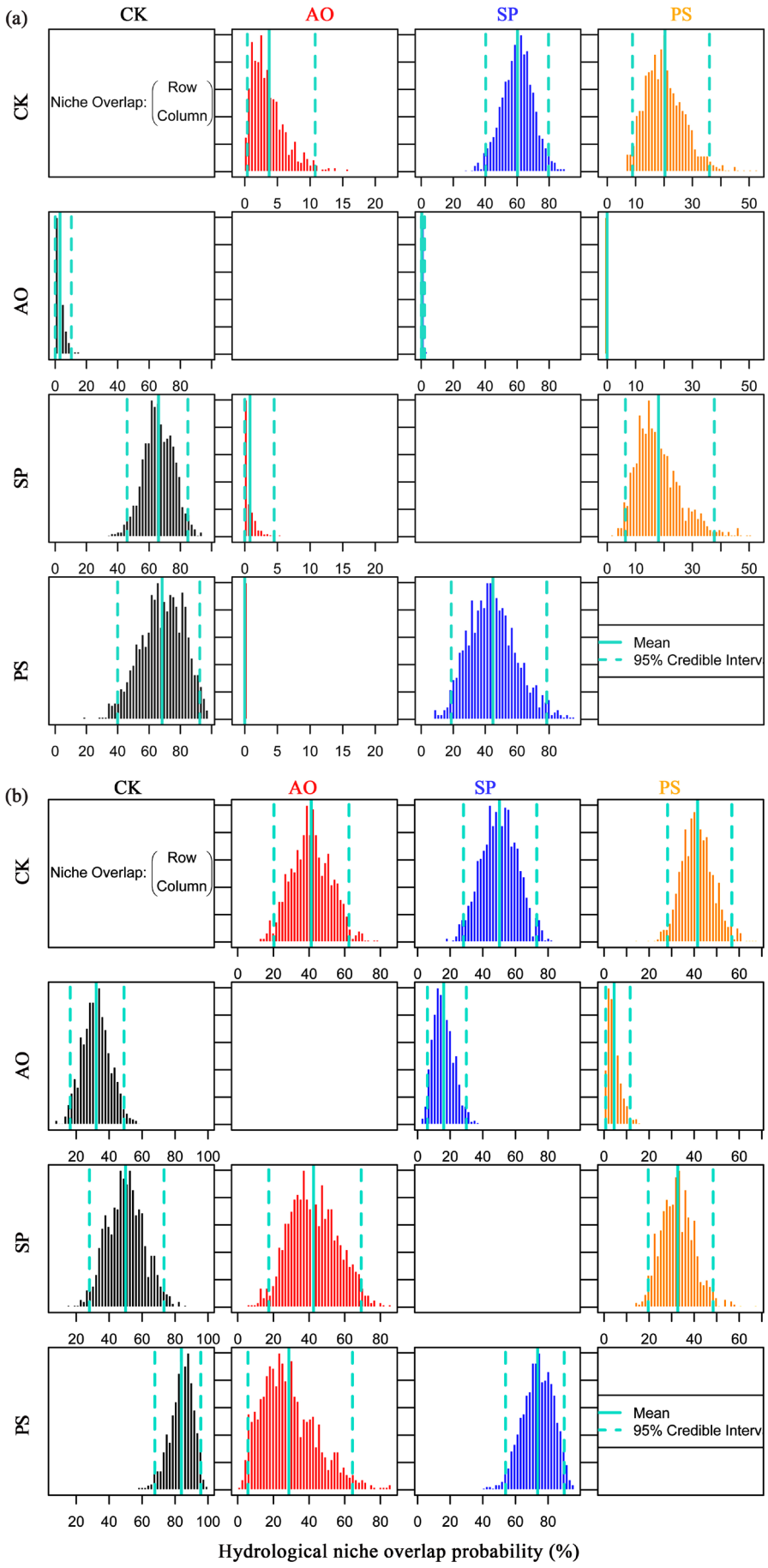
(a)
CK
AO
SP
PS
Niche Overlap:
Row
Column
Mean
95% Credible Interv
(b)
Hydrological niche overlap probability (%)

841

Fig. S2 Posterior distribution of the probabilistic niche overlap metric (%) for a specified N_R of 95% in 2018 (a) and 2019 (b). The posterior means and 95% credible intervals are displayed in green. The numbers in the plots indicate the mean probability that an individual from the species indicated by row will be found within the niche of the species indicated by the column header. The four species displayed are *C. korshinskii* (CK), *A.ordosica* (AO), *S.psammophila* (SP) and *P. simonii* (PS).

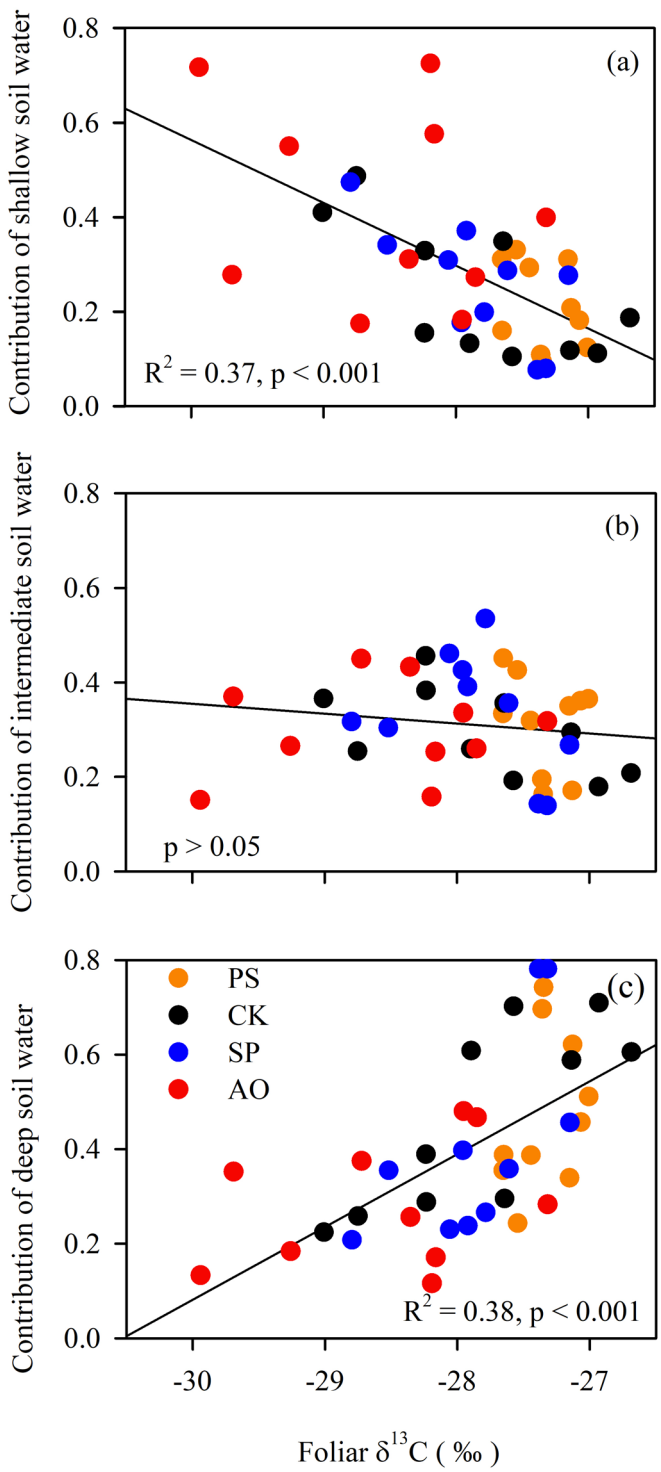

Fig. S3 Relationships between contribution of shallow soil water (a), intermediate soil water (b), deep soil water (c) and foliar $\delta^{13}C$ of four species (CK, *C. korshinskii*; AO, *A.ordosica*; SP, *S.psammophila*; PS, *P. simonii*, N=10 per species).

Table S1 Mean probabilistic niche overlap (%) among the four plant species in the wet year (2018) using δ^2H and $\delta^{18}O$.

	A. ordosica	*C. korshinskii*	*P. simonii*	*S. psammophila*
A. ordosica	NA	7	6	22
C. korshinskii	26	NA	74	79
P. simonii	42	91	NA	95
S. psammophila	63	73	67	NA

Note: the numbers indicate the probability that an individual from the species indicated by row will be found within the niche of the species indicated by the column header.